Hybrid Control Law for a Three-Level NPC Rectifier

Sabrina Hadjeras, Carolina Albea Sanchez, F Gomez-Estern Aguilar, F Gordillo, Germain Garcia

Hybrid Control Law for a Three-Level NPC Rectifier

S. Hadjeras, C. Albea Sanchez, F. Gomez-Estern Aguilar, F. Gordillo and G. Garcia

***Abstract*— In this article, a hybrid control law is proposed for the three-phase three-level Neutral Point Clamped (NPC) converter working as a rectifier in order to regulate the output DC voltage. The control problem deals with the unbalance capacitor voltages as well as the phase currents. The proposed algorithm is based on the Hybrid Dynamical System theory, which takes into account the hybrid nature of the NPC converter, i.e., the continuous and discrete dynamics, ensuring uniform global asymptotic stability of the operating point. Finally, the effectiveness of the proposed control algorithm is validated in simulation.**

***Index Terms*— Three-phase three-level neutral point clamped converter, rectifier, hybrid dynamical system, nonlinear time-varying system.**

I. Introduction

During the last decades, the control of multilevel power converters has been widely studied in the literature, since they can achieve high power using mature medium-power semiconductor technology and present more advantages compared with conventional ones. These advantages are the output signal quality and a nominal power increase in the converter [1]. Particularly, the control of three-phase, three-level Neutral Point Clamped (NPC) converter, well-known as AC/DC rectifier proposed by [2], has attracted a lot of attention. From the electronic community, it is one of the most used multilevel power converter for AC/DC conversion (DC motor drives, battery charging systems, appliances [1][3]) due to its high power rating and its lower total harmonic distortion. From the control community, the control design of such system is recognized to be a challenging task, since the dynamical behavior can be modeled as a nonlinear time-varying and hybrid system. Indeed, voltages and currents are continuous-time signals, whereas the control signals are generated by switches devices, which are consequently of a discrete nature. This fact makes the control design a complex task.

The main control objectives of this class of system are twofold. Firstly, we aim to obtain desired sinusoidal input currents. Secondly, we desire to generate a dc link voltage keeping it constant at the desired reference value, while maintaining the neutral point voltage close to zero. In order to achieve these control objectives, some control strategies have been developed. A first classical approach widely studied relies on the control design of averaged models [4][5]. The most employed averaged controller for the NPC rectifier is called Direct Power Control (DPC) method. This approach uses generally two or more PI controllers, one for the instantaneous powers, the second one to keep the neutral point voltage close to zero and the third one to regulate the dc-link voltage to a desired value [6][7].

Recently, some control strategies have been proposed to directly control the switches without considering an averaged model, which led to discontinuous control laws. Among them, we can cite predictive control algorithms (for inverters in [8] and converters in [9]), sliding mode controllers (for inverters in [10][11] and converters in [12][13]) and hybrid controllers (for inverters in [14] and converters in [15]). For the case of the NPC, to the best of our knowledge, only a few papers have considered explicitly the discrete nature of the switches. In [16][17], a predictive control algorithm is used to predict the capacitor voltages for the next sampling time. In [18] a sliding mode control design is considered and the sliding surfaces use directly the error between the state variables and their references.

In this work, we propose to model the NPC as a hybrid model by considering, the voltage and current signals as continuous dynamics, as well as, the switching signals as discrete dynamics. However, the challenge in this article is to consider the nonlinear time-varying nature of the system. Following the Hybrid Dynamical System (HDS) theory [19], we propose a control guaranteeing Uniform Global Asymptotic Stability (UGAS) of the operating point.

This paper is organized as follows: In section II, a first model for the NPC is proposed in *abc* coordinates, afterward, this model is transformed into $\alpha\beta\gamma$ coordinates, and a coordinate change is introduced in order to consider the active and reactive powers instead of phase currents. Important assumptions, properties and control problems are stated in this section. Section III proposes the model using the hybrid framework, and describes the hybrid control law ensuring stability properties using the HDS theory. Some simulations are performed in section IV. Finally, the conclusion of the proposed work is addressed in Section V.

Notation: Throughout the paper, $\mathbb{R}$ denotes the set of real numbers, $\mathbb{R}^n$ the n-dimensional Euclidean space and

S. Hadjeras and C. Albea Sanchez are with LAAS-CNRS, Université de Toulouse, CNRS, UPS, Toulouse France. shadjera,calbea@laas.fr

F. Gomez-Estern Aguilar is with Universidad Loyola Andalucía Seville Spain. fgestern@uloyola.es

F. Gordillo is with Universidad of Seville, Seville Spain. gordillo@us.es

G. Garcia is with both LAAS-CNRS, Université de Toulouse, CNRS, INSA, Toulouse France. garcia@laas.fr

$\mathbb{R}^{n\times m}$ the set of all real $m \times n$ matrices. We denote with 1_4 the identity matrix $\mathbb{R}^{4\times4}$. The set $\mathcal{S}^n$ denotes the set of symmetric positive definite matrices of matrices $\mathbb{R}^{n\times n}$. The symbol $\langle .,. \rangle$ denotes the standard Euclidean inner product and $\otimes$ define the Kronecker product.

II. Dynamical model of the NPC rectifier

A. The NPC architecture and dynamical modeling

The considered system is a three-phase three-level NPC converter working as a rectifier [2], whose structure is depicted in Figure 1. This converter is connected to the grid through inductors, L, and parasitic resistances, R_{LS}. These parasitic resistances model not only the resistive components of the inductance, but also the dissipated switching energy. The phase voltages and the phase currents are denoted by v_{sa}, v_{sb}, v_{sc} and i_a, i_b, i_c, respectively. The *dc* link contains two capacitors C_1 and C_2, which are assumed to have the same value $C_1 = C_2 = C$ and whose respective voltages are denoted by v_{c_1} and v_{c_2}. The parasitic resistances R_{p_1} and R_{p_2} for capacitors C_1 and C_2, respectively, are considered and assumed to have the same value, $R_{p_1} = R_{p_2} = R_p$. This *dc* link is also connected to a pure resistive load R, and the voltage across this load is denoted v_{dc}. This voltage is the sum of the capacitor voltages ($v_{dc} = v_{c_1} + v_{c_2}$).

The control inputs $d_{ij} \in \{0, 1\}$, with $i = \{a, b, c\}$ and $j = \{p, o, n\}$ are assumed to be discrete variables:

$$d_{ij} = \begin{cases} 1, & \text{if phase } i \text{ is connected to level } j \\ 0, & \text{else.} \end{cases}$$

Moreover, this control variables present the following constraint [20]:

$$d_{ip} + d_{io} + d_{in} = 1, \qquad \text{for} \quad i = \{a, b, c\}.$$

Assumption 1: We assume in the following that the phase voltages and currents are balanced, that is:

$$\begin{aligned} v_{sa} + v_{sb} + v_{sc} &= 0, \\ i_a + i_b + i_c &= 0. \end{aligned}$$

Then, considering Assumption 1 and Fig. 1, a model of the NPC converter in *abc* coordinates can be expressed as:

$$\begin{aligned}
L\frac{di_a}{dt} &= v_{sa} - R_{LS}i_a + \frac{2d_{an} - 2d_{ap} - d_{bn} + d_{bp} - d_{cn} + d_{cp}}{6}v_{dc} \\
&\quad + \frac{-2d_{an} - 2d_{ap} + d_{bn} + d_{bp} + d_{cn} + d_{cp}}{6}v_d \\
L\frac{di_b}{dt} &= v_{sb} - R_{LS}i_b - \frac{d_{an} - d_{ap} - 2d_{bn} + 2d_{bp} + d_{cn} - d_{cp}}{6}v_{dc} \\
&\quad + \frac{d_{an} + d_{ap} - 2d_{bn} - 2d_{bp} + d_{cn} + d_{cp}}{6}v_d \\
L\frac{di_c}{dt} &= v_{sc} - R_{LS}i_c - \frac{d_{an} - d_{ap} + d_{bn} - d_{bp} - 2d_{cn} + 2d_{cp}}{6}v_{dc} \\
&\quad + \frac{d_{an} + d_{ap} + d_{bn} + d_{bp} - 2d_{cn} - 2d_{cp}}{6}v_{dc} \\
C\frac{dv_{dc}}{dt} &= (d_{ap} - d_{an})i_a + (d_{bp} - d_{bn})i_b + (d_{cp} - d_{cn})i_c \\
&\quad - \left(\frac{2}{R} + \frac{1}{R_p}\right)v_{dc} \\
C\frac{dv_d}{dt} &= (d_{ap} + d_{an})i_a + (d_{bp} + d_{bn})i_b + (d_{cp} + d_{cn})i_c - \frac{1}{R_p}v_d,
\end{aligned}$$

where v_d represents the dc-link capacitor voltage difference ($v_d = v_{c_1} - v_{c_2}$). Notice that, v_{sa}, v_{sb}, v_{sc} are the grid voltage in the so-called *abc* coordinates. In order to take into account the balanced phase voltages and currents, the Clarke Transformation [6] is used to obtain the model in $\alpha\beta\gamma$ coordinates:

$$\begin{cases}
L\frac{di_\alpha}{dt} = v_{s\alpha} - R_{LS}i_\alpha - (d_{\alpha p} - d_{\alpha n})\frac{v_{dc}}{2} - (d_{\alpha p} + d_{\alpha n})\frac{v_d}{2} \\
L\frac{di_\beta}{dt} = v_{s\beta} - R_{LS}i_\beta - (d_{\beta p} - d_{\beta n})\frac{v_{dc}}{2} - (d_{\beta p} + d_{\beta n})\frac{v_d}{2} \\
C\frac{dv_{dc}}{dt} = (d_{\alpha p} - d_{\alpha n})i_\alpha + (d_{\beta p} - d_{\beta n})i_\beta - (\frac{2}{R} + \frac{1}{R_p})v_{dc} \\
C\frac{dv_d}{dt} = (d_{\alpha p} + d_{\alpha n})i_\alpha + (d_{\beta p} + d_{\beta n})i_\beta - \frac{1}{R_p}v_d,
\end{cases} \tag{1}$$

where the control inputs $d_{\alpha p}$, $d_{\alpha n}$, $d_{\beta p}$ and $d_{\beta n}$ are the transformed of the control inputs $d_{ij} \in \{0, 1\}$, with $i = \{a, b, c\}$ and $j = \{p, o, n\}$, given before. Notice that the control inputs $d_{\gamma j}$ and d_{io} do not appear in this model.

The voltage variables, $v_{s\alpha}$ and $v_{s\beta}$, and the current variables, i_α and i_β, are the transformations in $\alpha\beta\gamma$ of the phase voltages and phase currents, respectively. Notice that, according to Assumption 1, as the phase voltages and phase currents are assumed to be balanced, then the last transformation leads to:

$$\begin{aligned} v_\gamma &= 0 \\ i_\gamma &= 0. \end{aligned}$$

B. Modeling of the input voltage $v_{s\alpha}$ and $v_{s\beta}$

The grid voltages in $\alpha\beta\gamma$ coordinates are expressed as follows:

$$\begin{cases} v_{s\alpha}(t) = V_{s\alpha}\sin(wt) \\ v_{s\beta}(t) = V_{s\beta}\cos(wt), \end{cases} \tag{2}$$

where $V_{s\alpha}$, $V_{s\beta}$ and w are, respectively, the amplitude and the frequency of the grid voltage. We assume in the following that $V_{s\alpha} = V_{s\beta} = V_s$.

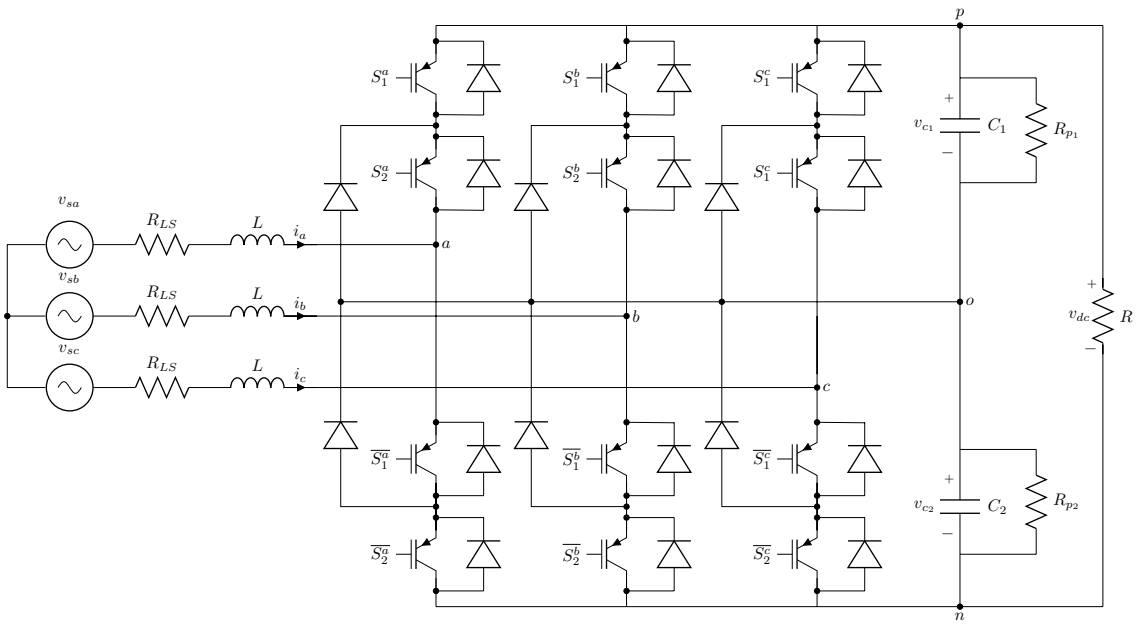

Fig. 1. Three-phase three-level neutral point clamped (NPC) rectifier.

Remark 1: Note that from (2), it is simple to deduce that

$$v_{s\alpha}^2(t) + v_{s\beta}^2(t) = V_s^2.$$

We can therefore define the following set

$$\Phi = \{(v_{s\alpha}(t), v_{s\beta}(t)) \in \mathbb{R}^2, \quad v_{s\alpha}^2(t) + v_{s\beta}^2(t) = V_s^2\}. \quad (3)$$

As depicted in Fig. 2, the set (3) can be embedded into a polytope described as:

$$\Omega := \sum_{j=1}^{4} \nu_j \Omega_j \quad \text{for} \quad 0 \leq \nu_j \leq 1 \quad \text{and} \quad \sum_{j=1}^{4} \nu_j(t) = 1,$$

where Ω_j $(j = 1, 2, 3, 4)$ represents the vertices of the polytope in the $(v_{s\alpha}, v_{s\beta})$-plane:

$\Omega_1 = \begin{bmatrix} V_{s\alpha} \\ V_{s\beta} \end{bmatrix}$, $\Omega_2 = \begin{bmatrix} -V_{s\alpha} \\ V_{s\beta} \end{bmatrix}$, $\Omega_3 = \begin{bmatrix} V_{s\alpha} \\ -V_{s\beta} \end{bmatrix}$, $\Omega_4 = \begin{bmatrix} -V_{s\alpha} \\ -V_{s\beta} \end{bmatrix}$.

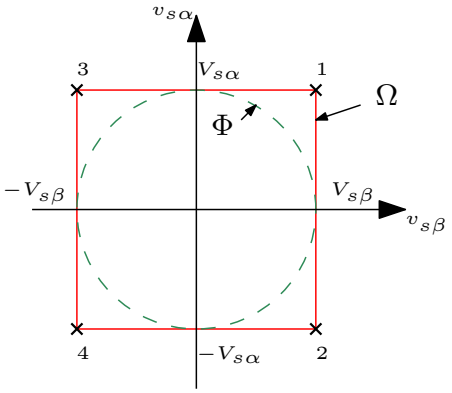

Fig. 2. Representation of a set (3) and the proposed polytope.

C. The NPC dynamical model based on instantaneous powers

The control algorithm is easier to express using instantaneous powers instead of current variables [21]. Furthermore, phase currents i_α and i_β can be also expressed in terms of instantaneous active and reactive powers [22]:

$$i_\alpha = \frac{1}{V_s^2}(v_{s\alpha}(t)p - v_{s\beta}(t)q) \quad (4)$$

$$i_\beta = \frac{1}{V_s^2}(v_{s\beta}(t)p + v_{s\alpha}(t)q) \quad (5)$$

where p and q represent the instantaneous active and reactive powers of the system, respectively.

Then, model (1) can be rewritten according to the new state variable $x = [p \; q \; v_{dc} \; v_d]^T$:

$$\dot{x} = \overbrace{\begin{bmatrix} -\frac{R_{LS}}{L} & 2\pi f & -\frac{\xi_1}{2L} & -\frac{\xi_3}{2L} \\ -2\pi f & -\frac{R_{LS}}{L} & \frac{\xi_2}{2L} & \frac{\xi_4}{2L} \\ \frac{\xi_1}{CV_s^2} & -\frac{\xi_2}{CV_s^2} & -(\frac{2}{RC} + \frac{1}{R_pC}) & 0 \\ \frac{\xi_3}{CV_s^2} & -\frac{\xi_4}{CV_s^2} & 0 & -\frac{1}{R_pC} \end{bmatrix}}^{A_u(t)} x + \overbrace{\begin{bmatrix} \frac{V_s^2}{L} \\ 0 \\ 0 \\ 0 \end{bmatrix}}^{B}, \quad (6)$$

where, f is the frequency of the phase voltages, and

$$\xi_1 = u_1 v_{s\alpha}(t) + u_2 v_{s\beta}(t), \qquad \xi_2 = u_1 v_{s\beta}(t) - u_2 v_{s\alpha}(t),$$
$$\xi_3 = u_3 v_{s\alpha}(t) + u_4 v_{s\beta}(t), \qquad \xi_4 = u_3 v_{s\beta}(t) - u_4 v_{s\alpha}(t).$$

These equations can be rewritten as follows:

$$\xi = \begin{bmatrix} \Gamma & 0 \\ 0 & \Gamma \end{bmatrix} u. \quad (7)$$

with $\xi = [\xi_1 \quad \xi_2 \quad \xi_3 \quad \xi_4]^T$ and $\Gamma = \begin{bmatrix} v_{s\alpha}(t) & v_{s\beta}(t) \\ v_{s\beta}(t) & -v_{s\alpha}(t) \end{bmatrix}$.
$u = [u_1 \quad u_2 \quad u_3 \quad u_4]^T$ is a vector containing the control

variables

$$u_1 = d_{\alpha p} - d_{\alpha n} \qquad u_2 = d_{\beta p} - d_{\beta n}$$
$$u_3 = d_{\alpha p} + d_{\alpha n} \qquad u_4 = d_{\beta p} + d_{\beta n}.$$

At this stage, let consider vector $u = [u_1\ u_2\ u_3\ u_4]^T$ with $u \in U$, where U is a set of all possible combinations for the control inputs. For the considered synchronous rectifier, there are 27 possible combinations of the switches [6], but as there are redundant switching states, we only need to consider 25 combinations, meaning that $u \in \{u^{(1)}, ..., u^{(25)}\}$ with $u \in \mathbb{R}^4$. Note that, the model (6) is nonlinear time-variant system.

To ease the stability analysis, a new formulation of this nonlinear time-varying system is proposed, based on a polytopic presentation. First of all, notice that the matrix Γ defined in (7) can be written as a polytope:

$$\Gamma = \sum_{j=1}^{4} \mu_j(t)\Gamma_j,$$

where $\mu_j(t) \in [0, 1]$ is a function satisfying $\sum_{j=1}^{4} \mu_j(t) = 1$ and Γ_j are defined as

$$\Gamma_1 = \begin{bmatrix} V_{s\alpha} & V_{s\beta} \\ V_{s\beta} & -V_{s\alpha} \end{bmatrix}, \qquad \Gamma_2 = \begin{bmatrix} -V_{s\alpha} & V_{s\beta} \\ V_{s\beta} & V_{s\alpha} \end{bmatrix}$$
$$\Gamma_3 = \begin{bmatrix} V_{s\alpha} & -V_{s\beta} \\ -V_{s\beta} & -V_{s\alpha} \end{bmatrix}, \qquad \Gamma_4 = \begin{bmatrix} -V_{s\alpha} & -V_{s\beta} \\ -V_{s\beta} & V_{s\alpha} \end{bmatrix}.$$

Then, equation (7) can be written as:

$$\xi = \sum_{j=1}^{4} \mu_j(t) \begin{bmatrix} \Gamma_j & 0 \\ 0 & \Gamma_j \end{bmatrix} u.$$

Matrix $A_u(t)$ defined in system (6), can also be written as follows:

$$A_u(t) = \sum_{j=1}^{4} \mu_j(t) A_u(j), \tag{8}$$

where

$$A_u(j) = \begin{bmatrix} M_1 & M_2 & M_3 & M_4 \end{bmatrix} \left(\begin{bmatrix} \Gamma_j & 0 \\ 0 & \Gamma_j \end{bmatrix} u \right) \otimes 1_4 + M_0 \tag{9}$$

and

$$M_0 = \begin{bmatrix} -\frac{R_{LS}}{L} & 2\pi f & 0 & 0 \\ -2\pi f & -\frac{R_{LS}}{L} & 0 & 0 \\ 0 & 0 & -(\frac{2}{RC} + \frac{1}{R_p C}) & 0 \\ 0 & 0 & 0 & -\frac{1}{R_p C} \end{bmatrix}$$

$$M_1 = \begin{bmatrix} 0 & 0 & -\frac{1}{2L} & 0 \\ 0 & 0 & 0 & 0 \\ \frac{1}{CV_s^2} & 0 & 0 & 0 \\ 0 & 0 & 0 & 0 \end{bmatrix}, \ M_2 = \begin{bmatrix} 0 & 0 & 0 & 0 \\ 0 & 0 & \frac{1}{2L} & 0 \\ 0 & -\frac{1}{CV_s^2} & 0 & 0 \\ 0 & 0 & 0 & 0 \end{bmatrix}$$

$$M_3 = \begin{bmatrix} 0 & 0 & 0 & -\frac{1}{2L} \\ 0 & 0 & 0 & 0 \\ 0 & 0 & 0 & 0 \\ \frac{1}{CV_s^2} & 0 & 0 & 0 \end{bmatrix}, \ M_4 = \begin{bmatrix} 0 & 0 & 0 & 0 \\ 0 & 0 & 0 & \frac{1}{2L} \\ 0 & 0 & 0 & 0 \\ 0 & -\frac{1}{CV_s^2} & 0 & 0 \end{bmatrix}.$$

Consequently, the original nonlinear model (6) can be rewritten as a polytopic system as follows:

$$\dot{x} = \sum_{j=1}^{4} \mu_j(t) A_u(j) x + B. \tag{10}$$

The next assumption is necessary to guarantee the existence of a switching signal that ensures forward invariance of the equilibrium point, x_e, in the generalized sense of Filippov, considering $u \in \{u^{(1)}, ..., u^{(25)}\}$ and equation (8).

Assumption 2: There exist 25 functions of time $\lambda_{1_{eq}}(t), \lambda_{2_{eq}}(t), ..., \lambda_{25_{eq}}(t)$ satisfying $\sum_{l=1}^{25} \lambda_{i_{eq}}(t) = 1$ for all $t > 0$, such that the following convex combination holds for every t:

$$\sum_{l=1}^{25} \lambda_{l_{eq}}(t)(A_{u^{(l)}}(t)x_e + B) = 0, \tag{11}$$

with

$$A_{u^{(l)}}(t) = \begin{bmatrix} M_1 & M_2 & M_3 & M_4 \end{bmatrix} \left(\begin{bmatrix} \Gamma & 0 \\ 0 & \Gamma \end{bmatrix} u^{(l)} \right) \otimes 1_4 + M_0$$

where $u^{(l)} \in U$ and x_e is the desired value of the regulation, meaning that the equilibrium point is reached in sense of Filippov.

In order to establish the stability properties of the equilibrium point x_e, we introduce the following property.

Property 1: For matrices $A_u(j)$ defined in (9), there exist common matrices $P, Q \in \mathcal{S}^4$ satisfying

$$A_{u^{(i)}}(j)^T P + P A_{u^{(i)}}(j) + 2Q < 0, \tag{12}$$

for all $j \in \{1, ..., 4\}$ and $u^{(i)} \in U$ with $i \in \{1, ..., 25\}$. Therefore, matrices $A_{u^{(i)}}(j)$ are Hurwitz.

Proof: The statement can be easily proved choosing

$$P = \begin{bmatrix} L & 0 & 0 & 0 \\ 0 & L & 0 & 0 \\ 0 & 0 & CV_s^2 & 0 \\ 0 & 0 & 0 & CV_s^2 \end{bmatrix},$$

$$Q = \begin{bmatrix} -R_{LS} & 0 & 0 & 0 \\ 0 & -R_{LS} & 0 & 0 \\ 0 & 0 & -(\frac{1}{R} + \frac{1}{2R_p})V_s^2 & 0 \\ 0 & 0 & 0 & -\frac{g}{2R_p} \end{bmatrix},$$

which are found from the system structure and energy-like arguments. ■

D. The control objectives

The objectives of the control problem are summarized as follows:

1) The instantaneous active power p and the instantaneous reactive power q should track their references denoted p^* and q^*, respectively,

$$p \to p^*$$
$$q \to q^*.$$

2) The sum of the converter capacitors voltages v_{dc} should be regulated towards its reference denoted v_{dc}^*,

$$v_{dc} \to v_{dc}^*.$$

3) The difference of the converter capacitors voltages v_d should be as small as possible,

$$v_d \to 0.$$

Then, the desired equilibrium point can be represented as $x_e = [x_{e1} \;\; x_{e2} \;\; x_{e3} \;\; x_{e4}]^T = [p^* \;\; q^* \;\; v_{dc}^* \;\; 0]^T$.

In order to achieve these objectives, while taking into account the real nature of the system, we propose a control algorithm described in the next section.

III. Hybrid model and proposed control law

Continuous-time and discrete-time dynamics are present in the considered system and the HDS theory developed in [19] is a natural way to take both dynamics into consideration. The continuous evolution (or flows) represents the evolution of the instantaneous active and reactive power states and the voltages v_{dc} and v_d. Likewise, the discrete evolution (or jumps) represents switching control inputs $u \in \{u^{(1)}, ..., u^{(25)}\}$.

Then, the closed loop system can be modeled easily as a hybrid of the form $\mathcal{H} = (\mathcal{C}, f, \mathcal{D}, G)$:

$$\mathcal{H} : \begin{cases} \begin{bmatrix} \dot{x} \\ \dot{u} \end{bmatrix} &= f(x,u), \qquad (x,u) \in \mathcal{C}, \\ \begin{bmatrix} x^+ \\ u^+ \end{bmatrix} &\in G(x,u), \qquad (x,u) \in \mathcal{D}, \end{cases} \tag{13}$$

$$\begin{aligned} f(x,u) &:= \begin{bmatrix} A_u(t)x + B \\ 0 \end{bmatrix}, \\ G(x,u) &:= \begin{bmatrix} x \\ \underset{i \in \mathbb{K}}{\operatorname{argmin}} \; \tilde{x}^T P (A_{u^{(i)}}(t)x + B) \end{bmatrix} \end{aligned} \tag{14}$$

with $i \in \{1, 2, ..., 25\}$ and $\tilde{x} = x - x_e$ the error between x and the equilibrium x_e.

The flow and jump set are given as:

$$\mathcal{C} := \{(x,u) : \tilde{x}^T P (A_u(t)x + B) \leq -\eta \tilde{x}^T Q \tilde{x}\}, \tag{15}$$

$$\mathcal{D} := \{(x,u) : \tilde{x}^T P (A_u(t)x + B) \geq -\eta \tilde{x}^T Q \tilde{x}\}, \tag{16}$$

where $\eta \in (0,1)$ is a design parameter.

The basic idea used in model (13)-(16) is as follows: assume there exists a common Lyapunov function, $V = x^T P x$, for all modes of the system, then

- if the Lyapunov function is sufficiently decreasing for a given control input, then this value of control is maintained.
- If the derivative of the Lyapunov function is not sufficiently negative, the control input is changed in order to improve the decreasing of V.

Remark 2: Note that, parameter η can adjust the switching frequency. Indeed, by decreasing η, we reduce the switching frequency and on the contrary, by increasing η, we raise the switching frequency. For practical reasons, the switching frequency must be low enough. Nevertheless, according to [15], this tuned parameter can manage some LQ performance.

Proposition 1: The hybrid system $(13) - (16)$ satisfies the following basic hybrid conditions given in [19, Assumption 6.5]:

- sets $\mathcal{C}$ and $\mathcal{D}$ given in (15) and (16) respectively, are closed.
- f is a continuous function, thus is therefore outer semicontinuous and it is also locally bounded. Moreover, f is convex for all $(x,u) \in \mathcal{C}$.
- G is outer semicontinuous [19, Definition 5.9] and locally bounded relative to $\mathcal{D}$.

Then, we can conclude that the hybrid system $(13) - (16)$ is well-posed.

The next Lemma guarantees the control mechanism described before, ensuring that the Lyapunov function is decreasing enough after each jump.

Lemma 1: Consider matrices $P, Q \in \mathcal{S}^4$ satisfying Property 1, a point $x_e \in \mathbb{R}^4$ satisfying Assumption 2, then, for each $x \in \mathbb{R}^4$,

$$\min_{i \in \mathbb{K}} \tilde{x}^T P (A_{u^{(i)}}(t)x + B) \leq -\tilde{x}^T Q \tilde{x}, \tag{17}$$

with $\tilde{x} = x - x_e$.

Proof: Considering the left hand side of (17), we get:

$$\begin{aligned} &\min_{i \in \mathbb{K}} \tilde{x}^T P (A_{u^{(i)}}(t)x + B) \\ &\leq \min_{i \in \mathbb{K}} \tilde{x}^T P A_{u^{(i)}}(t)\tilde{x} + \min_{i \in \mathbb{K}} \tilde{x}^T P (A_{u^{(i)}}(t)x_e + B). \end{aligned}$$

Using Property 1, we obtain that

$$\min_{i \in \mathbb{K}} \tilde{x}^T P A_{u^{(i)}}(t)\tilde{x} \leq -\tilde{x}^T Q \tilde{x}.$$

Following [23], $\min_{i \in \mathbb{K}} \tilde{x}^T P (A_{u^{(i)}}(t)x_e + B)$ can also be expressed as:

$$\begin{aligned} &\min_{i \in \mathbb{K}} \tilde{x}^T P (A_{u^{(i)}}(t)x_e + B) \\ &= \tilde{x}^T P \min_{\lambda_n \in [0,1]} \left(\sum_{n=1}^{25} \lambda_n(t)(A_{u_n}(t)x_e + B) \right) \\ &\leq \tilde{x}^T P \left(\sum_{n=1}^{25} \lambda_{neq}(t)(A_{u_n}(t)x_e + B) \right). \end{aligned}$$

Then, from Assumption 2, we obtain

$$\min_{i \in \mathbb{K}} \tilde{x}^T P (A_{u^{(i)}}(t)x_e + B) \leq 0, \tag{18}$$

which concludes the proof. ∎

Remark 3: We note here that, if $\tilde{x} \neq 0$

$$-\tilde{x}^T Q \tilde{x} < -\eta \tilde{x}^T Q \tilde{x}.$$

because $\eta < 1$.

Following the hybrid system theory, we will establish stability properties of the given compact set

$$\mathcal{A} := \{(x,u) : x = x_e, u \in U\}. \tag{19}$$

Theorem 1: Consider Assumption 2 and matrices $P, Q \in \mathcal{S}^4$ satisfying Property 1. Then, the set (19) is UGAS for hybrid system (13)–(16) for each x_e satisfying Assumption 2.

Proof: Let consider the Lyapunov function candidate $V(\tilde{x}) = \tilde{x}^T P \tilde{x}$, with $\tilde{x} = x - x_e$ which is continuously differentiable. Along the trajectories of the system (13)–(16)

- in the flow set, $\mathcal{C}$ (15), the derivative of $V(\tilde{x})$ is:

$$\langle \nabla V(\tilde{x}), f(\tilde{x},u)\rangle = \tilde{x}^T P(A_u(t)x + B) \leq -\eta \tilde{x}^T Q \tilde{x}. \tag{20}$$

- Moreover, in the jump set, $\mathcal{D}$ (16), the evolution of $V(\tilde{x})$ is :

$$V(\tilde{x}^+) - V(\tilde{x}) = \tilde{x}^T P \tilde{x} - \tilde{x}^T P \tilde{x} = 0. \tag{21}$$

We can remark that along the jumps, the strictly decreasing of the Lyapunov function is not guaranteed. Nevertheless, this property can be ensured applying [24, Theorem 1]. For this goal, we need to prove that system (13)–(16) presents semiglobal persistent flow.

Let us firstly build a restricted hybrid system $\mathcal{H}_{\delta,\Delta}$, corresponding to the intersection of the flow set $\mathcal{C}$ and the jump set $\mathcal{D}$ with the closed and bounded set:

$$S_{\delta,\Delta} = \{\tilde{x} :| \tilde{x} |\geq \delta \quad \text{and} \quad | \tilde{x} |\leq \Delta\}, \tag{22}$$

for each pair $0 < \delta < \Delta$ of positive scalars, and with the distance of x to the attractor (19) defined by $|x|_{\mathcal{A}} = |x - x_e| = |\tilde{x}|$. Notice that from the definition of (22), the solution $\tilde{x}$ is bounded. The restricted hybrid system $\mathcal{H}_{\delta,\Delta}$ is then defined as [24, eq.(3)]:

$$\mathcal{H}_{\delta,\Delta} := (\mathcal{C} \cap S_{\delta,\Delta}, f, \mathcal{D} \cap S_{\delta,\Delta}, G).$$

We can remark that, any solution to $\mathcal{H}_{\delta,\Delta}$ jumps to the interior of the flow bounded set $\mathcal{C} \cap S_{\delta,\Delta}$, Moreover, from Lemma 1, we get:

$$\tilde{x}^+(A_u(t)x^+ + B) \leq -\tilde{x}^{+^T} Q \tilde{x}^+ < -\eta \tilde{x}^{+^T} Q \tilde{x}^+ \tag{23}$$

with $\tilde{x}^+ = x^+ - x_e$, and from G in (14), after each jump $x^+ = x$, leading to $\tilde{x}^+ = x - x_e = \tilde{x}$. In (23), we get:

$$\tilde{x}(A_u(t)x + B) \leq -\tilde{x}^T Q \tilde{x} < -\eta \tilde{x}^T Q \tilde{x} \tag{24}$$

with $\tilde{x} \neq 0$, because $\tilde{x} \in S_{\delta,\Delta}$. This implies that the solutions must flow for some time after each jump. It also means that there is a strictly positive uniform dwell-time $\rho(\delta,\Delta)$ between each pair of consecutive jumps. Then, all assumptions of [24, Theorem 1] are satisfied, and UGAS of $\mathcal{A}$ is proven. ∎

IV. Simulations

In this section, some simulations are performed on the proposed closed loop system by using MATLAB/Simulink and by exploiting the HyEQ Toolbox [25] to verify the properties of the closed loop (13)–(16).
The parameters of the NPC are given in Table I. The simulations are made for different values of sampling time T_s (where the switching frequency is $f_s = \frac{1}{T_s}$). Moreover, we choose $\eta = 0.1$ following up the trade-off between switching frequency and performance mentioned in Remark 2.

TABLE I
Simulation parameters

Parameter	Convention	Value/Units
Estimated series resistance	R_{LS}	0.4 Ω
load resistance	R	30 Ω
Estimated parasitic resistance	R_p	20 $K\Omega$
Inductor	L	15 mH
Output capacitor	C	1500 μF
Total dc-link voltage reference	V^*_{dc}	150 V
Amplitude of the grid voltages	$V_{s\alpha}$	$62\sqrt{2}$ V
Grid frequency	f	50 Hz

The chosen matrix Q can achieve some LQ performance level, for example, reduce the levels of dissipated energy, following [15, Theorem 2]:

$$Q = \begin{bmatrix} 1 & 0 & 0 & 0 \\ 0 & 1 & 0 & 0 \\ 0 & 0 & 0.5 & 0 \\ 0 & 0 & 0 & 0.1 \end{bmatrix}.$$

Further, a common matrix P can be obtained such that Property 1 is satisfied:

$$P = \begin{bmatrix} 7.91 & 0 & 0 & 0 \\ 0 & 7.91 & 0 & 0 \\ 0 & 0 & 2773.78 & 0 \\ 0 & 0 & 0 & 3040.37 \end{bmatrix} \cdot 10^{-2}.$$

The desired equilibrium point is given as follows:

$$x_e = \begin{bmatrix} x_{1e} & 0 & V^*_{dc} & 0 \end{bmatrix}^T,$$

where x_{1e} is obtained from the equilibrium of model (6)

$$x_{1e} = \frac{2V_s^2 - V_s^2\sqrt{4 - \frac{8R_{LS}}{V_s^2}\left(\frac{2R_p+R}{R*R_p}\right)V^{*^2}_{dc}}}{4R_{LS}},$$

which is, $x_e = [782.4 \quad 0 \quad 150 \quad 0]^T$.

Figure 3 shows the evolution of states for different values of sampling time $T_s = \{10^{-4},\ 10^{-5},\ 10^{-6}\}s$. Note that, for these different values of T_s, the instantaneous active and reactive power, p and q, and the voltages v_{dc} and v_d converge, respectively, towards their desired references with a response time of to 0.02s. Furthermore, the instantaneous active and reactive powers signals admit a high-frequency ripple phenomenon due to switching control. Note that, when the switching frequency is

increased, then the ripple amplitude is reduced. Similar arguments are found for the phase currents, as shown in Figure 4, showing the trade-off between switching frequency and performance (if T_s increases, then the ripple signal increases). These simulations valid Theorem 1 statement.

Furthermore, the evolution of the Lyapunov function is depicted in Fig. 5, we can remark that when T_s is small then the steady state error of V is reduced. Likewise, when T_s is large, the Lyapunov function increases because we forbid the switches along period T_s.

Consequently, we can notice from the simulations that:

- the desired equilibrium point is reached in the generalized sense of Filippov as expected in Assumption. 2. It means that the desired equilibrium is generally obtained for a not constant control, meaning that the control switches between several values at an infinite switching frequency.
- In practical applications, as well as in simulation purposes, it is necessary to include a maximal switching frequency which has a significant impact on the quality of the convergence towards the desired equilibrium as shown in Fig. 3 and Fig. 4.
- If the switching frequency is reduced, then the difference between the balance and the state increases, and the ripple also increases. This phenomenon has not only been studied in the context of hybrid framework [26], but also in the problem of the discretization of the sliding mode control [27].

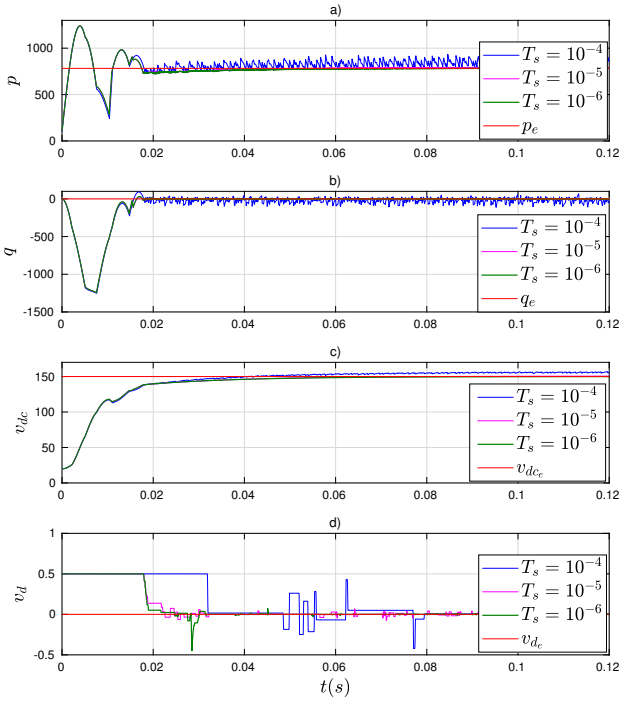

Fig. 3. Evolution of the states for different values of sampling time T_s and for $\eta = 0.1$.

V. Conclusions and Future work

In this article, we have considered a nonlinear time varying model of a three-phase three-level NPC converter. Furthermore, to ease the design of an efficient control law, a polytopic model is developed. Then a hybrid control scheme is proposed, ensuring that a desired attractor is UGAS for this hybrid closed loop system. Finally, the main result is validated in simulation.

Future works will be dedicated to ensure a practical global asymptotic stability including a minimum dwell-time in our hybrid scheme. Moreover, we expect to implement the control algorithm on a real system. The proposed control law needs also knowledge of the circuit parameters including the load resistance. Future work will include adaptive approaches to deal with this drawback.

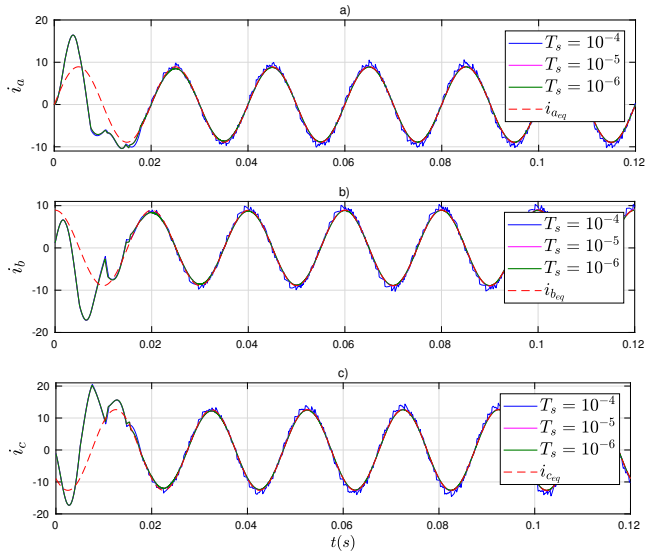

Fig. 4. Evolution of the phase currents for different values of sampling time T_s and for $\eta = 0.1$.

References

[1] J. I. Leon S. Kouro R. Portillo L. G. Franquelo, J. Rodriguez and M. A. M. Prats. The age of multilevel converters arrives. *IEEE Industrial Electronics Magazine*, 2(2):28–39, June 2008.

[2] I. Takahashi A. Nabae and H. Akagi. A new neutral-point-clamped pwm inverter. *IEEE Transactions on Industry Applications*, IA-17(5):518–523, Sept 1981.

[3] J. R. Espinoza J. Pontt J. R. Rodriguez, J. W. Dixon and P. Lezana. Pwm regenerative rectifiers: state of the art. *IEEE Transactions on Industrial Electronics*, 52(1):5–22, Feb 2005.

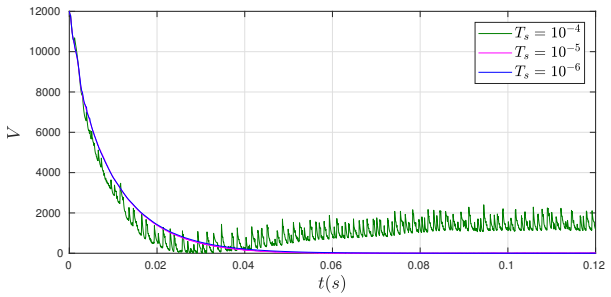

Fig. 5. Evolution of the Lyapunov function.

[4] K. Al-Haddad H. Kanaan and F. Fnaiech. Modelling and control of three-phase/switch/level fixed-frequency pwm rectifier: state-space averaged model. *IEE Proceedings - Electric Power Applications*, 152(3):551–557, May 2005.

[5] A. Yazdani and R. Iravani. A generalized state-space averaged model of the three-level npc converter for systematic dc-voltage-balancer and current-controller design. *IEEE Transactions on Power Delivery*, 20(2):1105–1114, April 2005.

[6] F. Gordillo F. Umbria and F. Salas. Model-based npc converter regulation for synchronous rectifier applications. In *IECON 2014 - 40th Annual Conference of the IEEE Industrial Electronics Society*, pages 4669–4675, Oct 2014.

[7] Y. Zhang Y. Zhang T. Lu, Z. Zhao and L. Yuan. A novel direct power control strategy for three-level pwm rectifier based on fixed synthesizing vectors. In *2008 International Conference on Electrical Machines and Systems*, pages 1143–1147, Oct 2008.

[8] Y. Cho I. Won and K. Lee. Predictive control algorithm for capacitor-less inverters with fast dynamic response. In *2016 IEEE International Conference on Power and Energy (PECon)*, pages 479–483, Nov 2016.

[9] L. Xie X. Li Z. Liu, F. Gao and L. Xie. Predictive functional control for buck dc-dc converter. In *The 27th Chinese Control and Decision Conference (2015 CCDC)*, pages 320–325, May 2015.

[10] D. Kalyanraj and S. L. Prakash. Design of sliding mode controller for three phase grid connected multilevel inverter for distributed generation systems. In *2016 21st Century Energy Needs - Materials, Systems and Applications (ICTFCEN)*, pages 1–5, Nov 2016.

[11] L. Hou Z. Liu X. Zheng, K. Qiu and C. Wang. Sliding-mode control for grid-connected inverter with a passive damped lcl filter. In *2018 13th IEEE Conference on Industrial Electronics and Applications (ICIEA)*, pages 739–744, May 2018.

[12] H. A. Bouziane M. B. Debbat and R. B. Bouiadjra. Sliding mode control of two-level boost dc-dc converter. In *2015 4th International Conference on Electrical Engineering (ICEE)*, pages 1–5, Dec 2015.

[13] C. S. Sachin and S. G. Nayak. Design and simulation for sliding mode control in dc-dc boost converter. In *2017 2nd International Conference on Communication and Electronics Systems (ICCES)*, pages 440–445, Oct 2017.

[14] C. Albea, O.L. Santos, D.A. Zambrano Prada, F. Gordillo, G. Garcia. Hybrid control scheme for a half-bridge inverter. In *IFAC 2017 World Congress*, July 2017.

[15] C. Albea, G. Garcia and L. Zaccarian. Hybrid dynamic modeling and control of switched affine systems: application to DC-DC converters. In *54th IEEE Conference on Decision and Control*, Osaka, Japan, December 2015.

[16] J. D. Barros and J. F. Silva. Optimal predictive control of three-phase npc multilevel converter for power quality applications. *IEEE Transactions on Industrial Electronics*, 55(10):3670–3681, Oct 2008.

[17] J. F. A. Silva J. D. Barros and E. G. A. Jesus. Fast-predictive optimal control of npc multilevel converters. *IEEE Transactions on Industrial Electronics*, 60(2):619–627, Feb 2013.

[18] V. Utkin Y. Alsmadi and L. Xu. Sliding mode control of ac/dc power converters. In *4th International Conference on Power Engineering, Energy and Electrical Drives*, pages 1229–1234, May 2013.

[19] R. Goebel, R.G. Sanfelice, and A.R. Teel. *Hybrid Dynamical Systems: modeling, stability, and robustness*. Princeton University Press, 2012.

[20] D. Borojevic H. Mao J. Bordonau, M. Cosan and F. C. Lee. A state-space model for the comprehensive dynamic analysis of three-level voltage-source inverters. volume 2, pages 942–948 vol.2, Jun 1997.

[21] M. Liserre F. Blaabjerg, R. Teodorescu and A. V. Timbus. Overview of control and grid synchronization for distributed power generation systems. *IEEE Transactions on Industrial Electronics*, 53(5):1398–1409, Oct 2006.

[22] Y. Kanazawa H. Akagi and A. Nabae. Generalized theory of the instantaneous reactive power in three-phase circuits. *Proceedings of the International Power Electronics Conference-IEEJ IPEC-Tokyo'83*, pages 1375–1386, 1983.

[23] F.S. Garcia G. S. Deaecto, J. C. Geromel and J.A. Pomilio. Switched affine systems control design with application to DC–DC converters. *IET control theory & applications*, 4(7):1201–1210, 2010.

[24] A. R. Teel C. Prieur and L. Zaccarian. Relaxed persistent flow/jump conditions for uniform global asymptotic stability. *IEEE Trans. on Automatic Control*, 59(10):2766–2771, October 2014.

[25] R. G. Sanfelice, D. Copp and P. A. Nanez. A toolbox for simulation of hybrid systems in Matlab/Simulink: Hybrid equations (HyEQ) toolbox. In *Hybrid Systems: Computation and Control Conference*, 2013.

[26] C. Albea Sanchez, G. Garcia, S. Hadjeras, M.W.P.M.H. Heemels, and L. Zaccarian. Practical stabilisation of switched affine systems with dwell-time guarantees. working paper or preprint, 2017.

[27] Z. Galias and X. Yu. Discretization effects in single input delayed sliding mode control systems. In *2013 European Conference on Circuit Theory and Design (ECCTD)*, pages 1–4, Sept 2013.